BIOCHEMICAL PHARMACOLOGY 75 (2008) 1717–1728

available at www.sciencedirect.com

ScienceDirect

journal homepage: www.elsevier.com/locate/biochempharm

An insight into the pharmacophores of phosphodiesterase-5 inhibitors from synthetic and crystal structural studies

Gong Chen [a,1], Huanchen Wang [b,1], Howard Robinson [c], Jiwen Cai [a], Yiqian Wan [a,*], Hengming Ke [b,**]

[a] School of Chemistry and Chemical Engineering, Center of Structure Biology, School of Pharmaceutical Sciences, Sun Yat-Sen University, Guangzhou 510275, PR China

[b] Department of Biochemistry and Biophysics, The University of North Carolina, Chapel Hill, NC 27599-7260, USA

[c] Biology Department, Brookhaven National Laboratory, Upton, NY 11973-5000, USA

ARTICLE INFO

Article history:
Received 24 October 2007
Accepted 24 January 2008

Keywords:
Phosphodiesterase (PDE)
Sildenafil
Viagra
Crystal structure

ABSTRACT

Selective inhibitors of cyclic nucleotide phosphodiesterase-5 (PDE5) have been used as drugs for treatment of male erectile dysfunction and pulmonary hypertension. An insight into the pharmacophores of PDE5 inhibitors is essential for development of second generation of PDE5 inhibitors, but has not been completely illustrated. Here we report the synthesis of a new class of the sildenafil derivatives and a crystal structure of the PDE5 catalytic domain in complex with 5-(2-ethoxy-5-(sulfamoyl)-3-thienyl)-1-methyl-3-propyl-1,6-dihydro-7*H*-pyrazolo[4,3-*d*]pyrimidin-7-one (**12**). Inhibitor **12** induces conformational change of the H-loop (residues 660–683), which is different from any of the known PDE5 structures. The pyrazolopyrimidinone groups of **12** and sildenafil are well superimposed, but their sulfonamide groups show a positional difference of as much as 1.5 Å. The structure–activity analysis suggests that a small hydrophobic pocket and the H-loop of PDE5 are important for the inhibitor affinity, in addition to two common elements for binding of almost all the PDE inhibitors: the stack against the phenylalanine and the hydrogen bond with the invariant glutamine. However, the PDE5–**12** structure does not provide a full explanation to affinity changes of the inhibitors. Thus alternatives such as conformational change of the M-loop are open and further structural study is required.

1. Introduction

Cyclic nucleotide phosphodiesterases (PDEs) are key enzymes that control cellular concentrations of the second messengers cAMP and cGMP [1–5]. The human genome encodes 21 PDE genes that are categorized into 11 families. Alternative mRNA splicing of the PDE genes produces about 100 isoforms of PDE proteins that distribute over various cellular compartments and play vital roles in physiological processes. PDE molecules contain a variable regulatory domain and a conserved catalytic domain. However, each PDE family shows characteristic substrate specificity and inhibitor selectivity. Family selective PDE inhibitors have been widely studied as therapeutics for treatment of various human diseases, including cardiotonics, vasodilators, smooth muscle relaxants, antidepressants, antithrombotics,

* *Corresponding author*. Tel.: +86 20 8411 0918.
** *Corresponding author*. Tel.: +1 919 966 2244; fax: +1 919 966 2852.
E-mail addresses: ceswyq@mail.sysu.edu.cn (Y. Wan), hke@med.unc.edu (H. Ke).
[1] These authors contributed equally to this work.
0006-2952/$ – see front matter
doi:10.1016/j.bcp.2008.01.019

antiasthmatics, and agents for improvement of learning and memory [6–14].

The most successful examples of this drug class are the PDE5 inhibitors (Fig. 1) sildenafil (Viagra), vardenafil (Levitra), and tadalafil (Cialis) that are drugs for treatment of male erectile dysfunction [7]. Sildenafil (Revatio) has additionally been approved for treatment of pulmonary hypertension [15]. Recently, udenafil (Zydena) has also been approved by Korean authorities for treatment of male erectile dysfunction [16]. Although four PDE5 inhibitors have been successfully approved as drugs for treatment of human diseases, enthusiasm for development of novel PDE5 inhibitors continues. In particular, PDE5 inhibitors have potential for other applications such as memory improvement, anticancer therapy, and treatment of heart diseases [13,17–20]. Thus, much recent attention has been given to development of second generation PDE5 inhibitors that have the same or different scaffolds as the current drugs but differ in their pharmacokinetic profiles [19].

Several structures of PDE5 in complex with various inhibitors are available [21–25]. However, an insight into the pharmacophores of PDE5 inhibitors, which is essential for development of the second generation of PDE5 inhibitors, has not been fully elucidated. For example, the structures of the PDE5 catalytic domain in complex with sildenafil or vardenafil showed an unfavorable interaction between these drugs and the invariant Gln817 that is an important residue for binding of substrate and inhibitors of all PDE families (Fig. 1). In particular, the distance between the amide oxygen of the Gln817 side chain and the ethoxyphenyl oxygen of sildenafil or vardenafil in the crystal structures [21,24,25] is typical of a hydrogen bond. However, both oxygen atoms involved in the contact lack a hydrogen donor for formation of a hydrogen bond. To explore the possibility of reducing this potentially unfavorable oxygen–oxygen opposition, we synthesized a series of PDE5 inhibitors in which the alkoxyphenyl ring of the scaffold is replaced with a five-membered thiophene ring, characterized the potency of the inhibitors, and determined a structure of the PDE5 catalytic domain in complex with the representative compound **12** (Fig. 1). The comparison of PDE5–**12** with the known structures of PDE5–inhibitor complexes provides insight into the pharmacophores of the PDE5 inhibitors and a structural basis for design of new second generation PDE5 inhibitors.

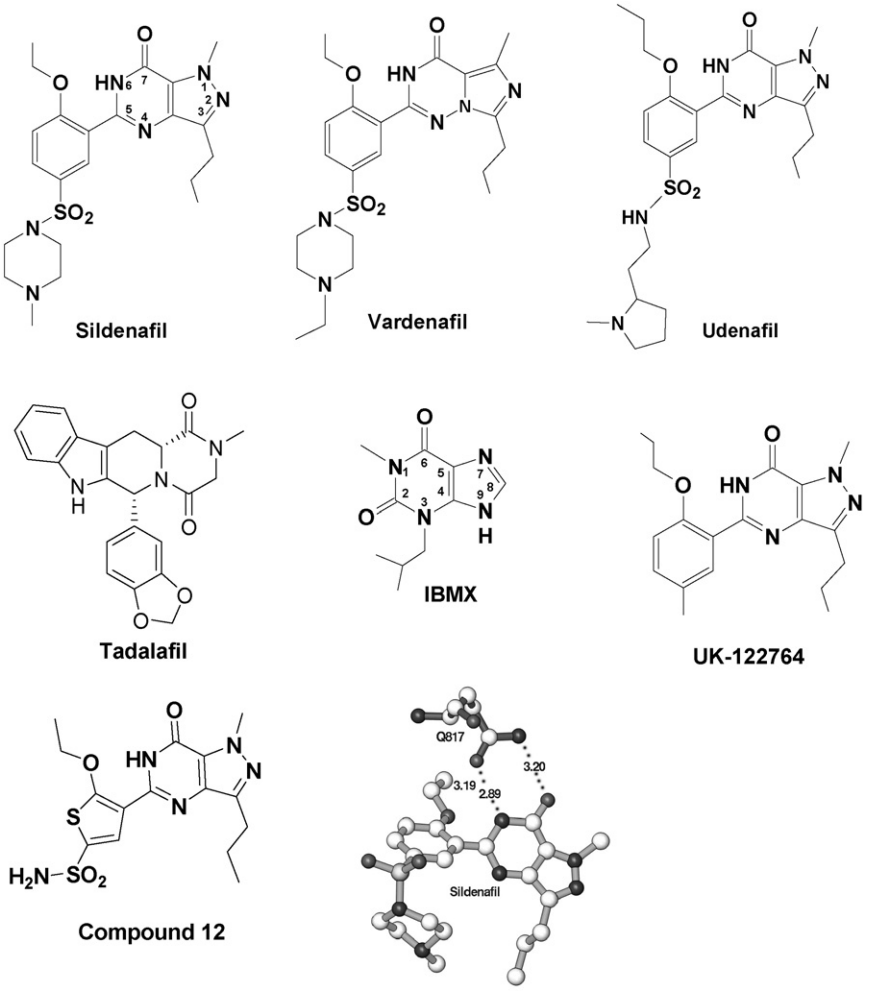

Fig. 1 – Chemical structures of the PDE5 inhibitors and the interaction of sildenafil with Gln817. Sildenafil, vardenafil, tadalafil and udenafil are drugs for treatment of erectile dysfunction. Compound 12 is an inhibitor synthesized for this study. IBMX is a non-selective inhibitor of most PDE families.

2. Materials and methods

2.1. Synthesis of PDE5 inhibitors

A series of sildenafil derivatives featuring a thiophene replacement for the phenyl group were synthesized using modified literature procedures (Scheme 1) [26–33].

2.1.1. 5-(2-Bromo-3-thienyl)-1-methyl-3-propyl-1,6-dihydro-7H-pyrazolo[4,3-d]pyrimidin-7-one (4) [26]

To a suspension of 2-bromothiophene-3-carboxylic acid (414 mg, 2.00 mmol) in anhydrous CH_2Cl_2 (20 mL) was added $SOCl_2$ (5 mL) and DMF (five drops). The mixture was refluxed for 4 h. After removal of the solvent and excess $SOCl_2$, the crude acyl chloride was suspended in pyridine (5 mL) and a solution of 4-amino-1-methyl-3-*n*-propylpyrazole-5-carboxamide hydrochloride (654 mg, 2.99 mmol) and Et_3N (606 mg, 5.99 mmol) in CH_2Cl_2 (10 mL) was added. After heating at reflux for 2 h, the reaction mixture was poured into cold water and extracted with 5% MeOH in CH_2Cl_2 (3× 50 mL). The organic extracts were combined, washed with water and brine, dried over Na_2SO_4, and evaporated to a dry solid in vacuo. The crude product was suspended in *t*-BuOH (25 mL) and *t*-BuOK (672 mg, 5.99 mmol) was added. The resulting mixture was heated at reflux under nitrogen for 4 h and then concentrated under vacuum and partitioned between CH_2Cl_2 and water. The organic layer was collected and the aqueous layer was further extracted with CH_2Cl_2 (2× 50 mL). The combined organic layer was dried over Na_2SO_4, concentrated under vacuum, and then purified by column chromatography (eluting with 2:1 Pet:EtOAc) to afford the title compound (317 mg, yield: 45%) as a white solid. mp 165–166 °C; ^{1}H NMR (300 MHz, CD_3SOCD_3): δ

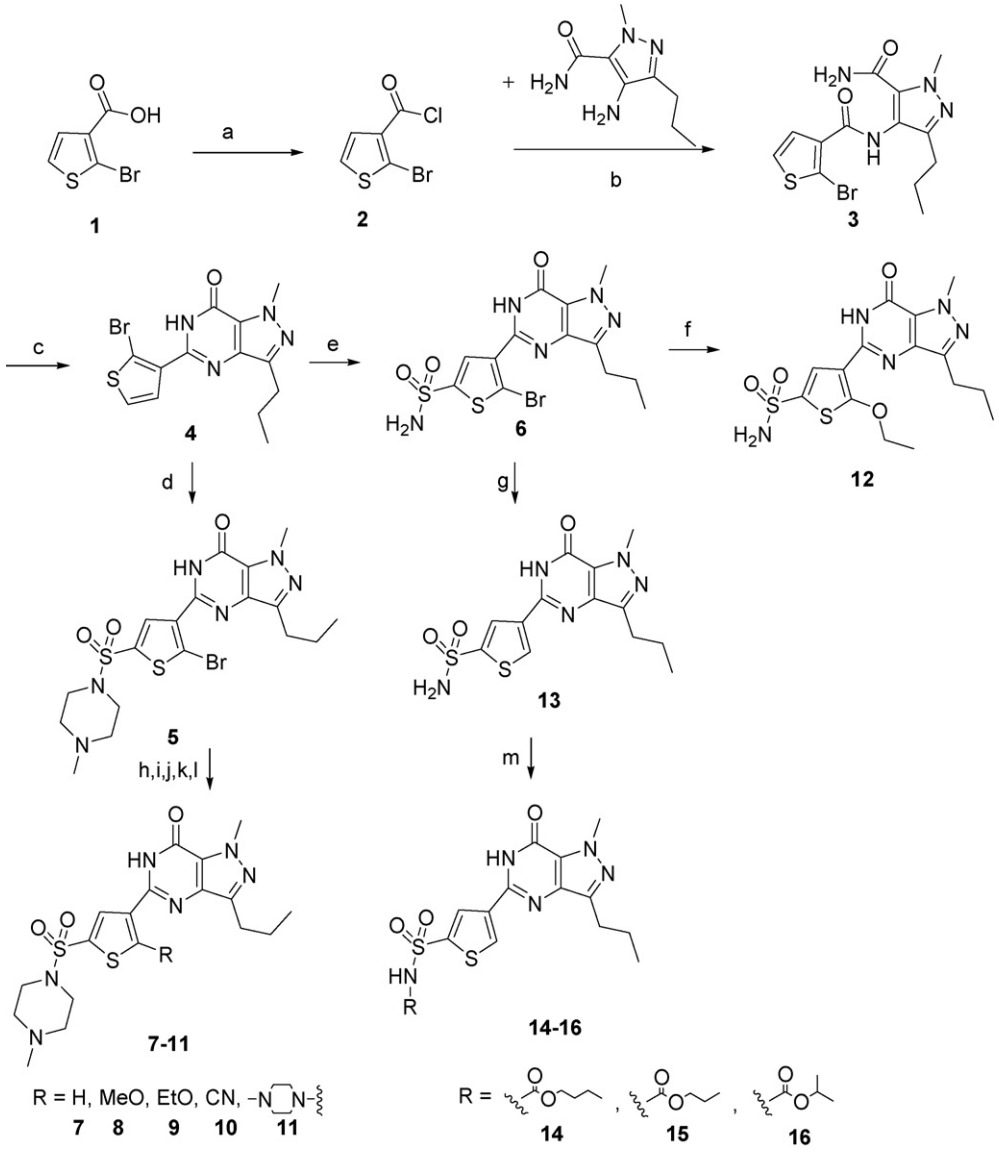

Scheme 1 – Synthesis of the compounds. Reagents and conditions: (a) $SOCl_2$, DMF, CH_2Cl_2, reflux; (b) pyridine, 70 °C; (c) *t*-BuOH, *t*-BuOK; (d) $ClSO_3H$, $SOCl_2$, *N*-methylpiperazine; (e) $ClSO_3H$, $SOCl_2$, aqueous ammonia; (f) EtONa, EtOH, reflux; (g and h) Zn dust; (i) CuI, MeONa, MeOH, reflux; (j) CuI, EtONa, EtOH, reflux; (k) CuCN, DMF, 150 °C; (l) $Pd(OAc)_2$, DPPF, Cs_2CO_3, *N*-methylpiperazine, 120 °C; (m) alkyl chloroformates (14–16), DMAP, pyridine, rt.

0.93 (t, J = 7.1, 3H, CH_3), 1.72–1.79 (m, 2H, CH_2), 2.76 (t, J = 7.2, 2H, CH_2), 4.14 (s, 3H, NCH_3), 7.32 (d, J = 5.5, 1H), 7.70 (d, J = 5.5, 1H), 12.34 (s, 1H); ^{13}C NMR (75 MHz, CD_3SOCD_3): δ 13.76, 21.59, 27.10, 37.77, 113.0, 124.1, 127.4, 128.5, 134.1, 137.2, 144.7, 145.4, 153.8; IR (KBr): 3434, 3152, 2965, 2928, 1693, 1591 cm^{-1}; ESI-MS: m/z = 351 $[M-H]^-$. Anal. calcd for $C_{13}H_{13}BrN_4OS$: C, 44.20; H, 3.71; N, 15.86; found: C, 44.38; H, 3.71; N, 15.87.

2.1.2. 5-(2-Bromo-5-(4-methylpiperazinylsulfonyl)-3-thienyl)-1-methyl-3-propyl-1,6-dihydro-7H-pyrazolo[4,3-d]pyrimidin-7-one (5) [27–29]

Compound **4** (177 mg, 0.50 mmol) was added to a mixture of thionyl chloride (1 mL) and chlorosulfonic acid (3 mL) cooled in an ice-water bath. The resultant mixture was heated to 40 °C with stirring for 2 h and then quenched by decanting onto ice (50 g). The aqueous mixture was extracted with $CHCl_3$ (2× 30 mL). The combined organic layer (containing the crude sulfonyl chloride of **4**) was concentrated to 25 mL under vacuum and triethylamine (155 mg, 1.53 mmol) and *N*-methylpiperazine (75 mg, 0.75 mmol) were added to the solution. The mixture was stirred overnight at room temperature. After removal of solvent, the residue was purified by column chromatography (eluting with 20:1 $CHCl_3$:CH_3OH) to afford the title compound (209 mg, yield: 81%) as a white solid.

mp 213–215 °C; ^{1}H NMR (300 MHz, CD_3SOCD_3): δ 0.93 (t, J = 7.2, 3H, CH_3), 1.72–1.80 (m, 2H, CH_2), 2.18 (s, 3H, NCH_3), 2.43 (br s, 4H), 2.77 (t, J = 7.2, 2H, CH_2), 3.04 (br s, 4H), 4.15 (s, 3H, NCH_3), 7.86 (s, 1H), 12.55 (br s, 1H); ^{13}C NMR (75 MHz, CD_3SOCD_3): δ 13.77, 21.61, 27.09, 37.81, 45.06, 45.65, 53.22, 120.4, 124.3, 133.1, 134.6, 135.0, 137.0, 144.1, 144.9, 153.7; IR (KBr): 3435, 2959, 2852, 1681, 1582 cm^{-1}; ESI-MS: m/z = 513 $[M-H]^-$. Anal. calcd for $C_{18}H_{23}BrN_6O_3S_2$: C, 41.94; H, 4.50; N, 16.30; found: C, 41.86; H, 4.60; N, 16.25.

2.1.3. 5-(2-Bromo-5-(sulfamoyl)-3-thienyl)-1-methyl-3-propyl-1,6-dihydro-7H-pyrazolo[4,3-d]pyrimidin-7-one (6)

The crude sulfonyl chloride of **4** was concentrated to 10 mL under vacuum and then added dropwise to cold concentrated ammonia solution (20 mL). The mixture was stirred at room temperature overnight. After removal of excess solvent, the crude product was collected by filtration and purified by column chromatography (eluted with $CHCl_3$:CH_3OH = 15:1). The yielded compound in title was a white solid (183 mg, yield: 85%).

mp 267–268 °C; ^{1}H NMR (300 MHz, CD_3SOCD_3): δ 0.93 (t, J = 7.2, 3H, CH_3), 1.71–1.78 (m, 2H, CH_2), 2.76 (t, J = 7.2, 2H, CH_2), 4.15 (s, 3H, NCH_3), 7.71 (s, 1H), 7.90 (br s, 2H, $SONH_2$), 12.52 (s, 1H); ^{13}C NMR (75 MHz, CD_3SOCD_3): δ 13.78, 21.64, 27.08, 37.81, 117.88, 124.3, 130.3, 134.4, 137.0, 144.5, 144.8, 145.3, 153.7; IR (KBr): 3434, 2960, 1676, 1581 cm^{-1}; ESI-MS: m/z = 432 $[M-H]^-$. Anal. calcd for $C_{13}H_{14}BrN_5O_3S_2$: C, 36.12; H, 3.26; N, 16.20; found: C, 36.05; H, 3.26; N, 16.38.

2.1.4. 5-(5-(4-Methylpiperazinylsulfonyl)-3-thienyl)-1-methyl-3-propyl-1,6-dihydro-7H-pyrazolo[4,3-d]pyrimidin-7-one (7) [27]

To a solution of compound **5** (60 mg, 0.12 mmol) in methanol (20 mL), zinc dust (23 mg, 0.36 mmol) and formic acid (0.2 mL) were added. The mixture was stirred overnight. Excess zinc dust was removed by filtration. The filtrate was concentrated in vacuum, then purified by column chromatography (eluted with $CHCl_3$:CH_3OH = 20:1). The yielded compound in title was a white solid (45 mg, yield: 85%).

mp 239–240 °C; ^{1}H NMR (300 MHz, CD_3SOCD_3): δ 0.95 (t, J = 6.8, 3H, CH_3), 1.72–1.79 (m, 2H, CH_2), 2.25 (s, 3H, NCH_3), 2.55 (br s, 4H), 2.79 (t, J = 6.9, 3H), 3.05 (br s, 4H), 4.14 (s, 3H, NCH_3), 8.20 (s, 1H), 8.78 (s, 1H), 12.54 (br s, 1H); ^{13}C NMR (125 MHz, CD_3SOCD_3): δ 13.70, 21.43, 26.93, 37.75, 45.03, 45.61, 53.21, 124.2, 131.5, 133.6, 135.5, 135.9, 137.3, 144.86, 144.91, 154.2; IR (KBr): 3418, 3093, 2934, 1682, 1578 cm^{-1}; ESI-MS: m/z = 435 $[M-H]^-$. Anal. calcd for $C_{18}H_{24}N_6O_3S_2$: C, 49.52; H, 5.54; N, 19.25; found: C, 49.67; H, 5.60; N, 19.13.

2.1.5. 5-(2-Methoxy-5-(4-methylpiperazinylsulfonyl)-3-thienyl)-1-methyl-3-propyl-1,6-dihydro-7H-pyrazolo[4,3-d]pyrimidin-7-one (8) [30]

After sodium (92 mg, 4.00 mmol) was completely dissolved in anhydrous methanol (20 mL), CuI (5 mg) and compound **5** (130 mg, 0.25 mmol) were added to the solution. The mixture was heated and refluxed in nitrogen for 6 h. The resulted mixture was concentrated under vacuum. The residue was partitioned between CH_2Cl_2 and water. The aqueous layer was further extracted with 5% MeOH in CH_2Cl_2 (2× 30 mL). The combined organic layer was dried over Na_2SO_4, concentrated in vacuum, and purified by column chromatography (eluted with $CHCl_3$:CH_3OH = 40:1). The yielded compound in title was a white solid (55 mg, yield: 47%).

mp 264–265 °C; ^{1}H NMR (300 MHz, $CDCl_3$): δ 1.03 (t, J = 7.2, 3H, CH_3), 1.79–1.87 (m, 2H, CH_2), 2.32 (s, 3H, NCH_3), 2.56 (br s, 4H), 2.89 (t, J = 7.2, 2H, CH_2), 3.20 (br s, 4H), 4.25 (s, 3H, NCH_3), 4.26 (s, 3H, OCH_3), 8.09 (s, 1H), 9.90 (s, 1H); ^{13}C NMR (75 MHz, $CDCl_3$): δ 14.13, 22.48, 27.72, 38.37, 45.74, 46.12, 53.98, 63.03, 115.3, 121.0, 124.1, 132.6, 138.1, 143.8, 146.6, 153.5, 167.7; IR (KBr): 3352, 2965, 1711, 1584 cm^{-1}; ESI-MS: m/z = 465 $[M-H]^-$. Anal. calcd for $C_{19}H_{26}N_6O_4S_2$: C, 48.91; H, 5.62; N, 18.01; found: C, 49.85; H, 5.70; N, 18.13.

2.1.6. 5-(2-Ethoxy-5-(4-methylpiperazinylsulfonyl)-3-thienyl)-1-methyl-3-propyl-1,6-dihydro-7H-pyrazolo[4,3-d]pyrimidin-7-one (9)

Compound **9** was prepared by the same method for compound **8**, except for a replacement of methanol with ethanol. It was a white solid (79 mg, yield: 66%).

mp 193–194 °C; ^{1}H NMR (300 MHz, CD_3SOCD_3): δ 0.93 (t, J = 7.2, 3H, CH_3), 1.44 (t, J = 6.3, 3H, CH_3), 1.71–1.78 (m, 2H, CH_2), 2.16 (s, 3H, NCH_3), 2.41 (br s, 4H), 2.75 (t, J = 7.2, 2H, CH_2), 3.00 (br s, 4H), 4.12 (s, 3H, NCH_3), 4.32–4.36 (m, 2H, OCH_2), 7.76 (s, 1H); ^{13}C NMR (75 MHz, CD_3SOCD_3): δ 13.78, 14.36, 21.51, 27.15, 37.69, 45.12, 45.68, 53.27, 72.40, 115.9, 118.1, 124.0, 132.3, 137.5, 144.3, 144.9, 154.2, 168.3; IR (KBr): 3363, 2930, 1699, 1588 cm^{-1}; ESI-MS: m/z = 481 $[M+H]^+$. Anal. calcd for $C_{20}H_{28}N_6O_4S_2$: C, 49.98; H, 5.87; N, 17.49; found: C, 49.85; H, 5.96; N, 17.38.

2.1.7. 5-(2-Cyano-5-(4-methylpiperazinylsulfonyl)-3-thienyl)-1-methyl-3-propyl-1,6-dihydro-7H-pyrazolo[4,3-d]pyrimidin-7-one (10) [31]

To a solution of compound **5** (65 mg, 0.13 mmol) in anhydrous DMF (5 mL), copper cyanide (17 mg, 0.19 mmol) was added. The resulted mixture was heated at 150 °C under nitrogen for

6 h, cooled to 100 °C, and poured into a solution of $FeCl_3{\cdot}6H_2O$ (81 mg, 0.300 mmol) in water and HCl. After heated to 60 °C for 20 min, the mixture was allowed to cool to room temperature and then extracted with 5% MeOH in CH_2Cl_2 (2× 50 mL). The combined organic layers were washed twice with water, dried over Na_2SO_4, concentrated in vacuum, and then purified by column chromatography (eluted with EtOAc:CH_3OH = 15:1). The yielded compound in title was a white solid (12 mg, yield: 20%).

mp 234–235 °C; ^{1}H NMR (300 MHz, CD_3SOCD_3): δ 0.92 (t, J = 7.0, 3H, CH_3), 1.77–1.84 (m, 2H, CH_2), 2.18 (s, 3H, NCH_3), 2.43 (br s, 4H), 2.79 (t, J = 7.0, 2H, CH_2), 3.11 (br s, 4H), 4.16 (s, 3H, NCH_3), 8.39 (s, 1H); ^{13}C NMR (75 MHz, CD_3SOCD_3): δ 13.59, 21.34, 27.12, 37.78, 44.98, 45.59, 53.20, 112.0, 112.1, 113.6, 130.9, 136.9, 141.3, 142.3, 143.0, 145.5, 153.9; IR (KBr): 3430, 2927, 2217, 1680, 1578 cm^{-1}; ESI-MS: m/z = 460 [M−H]$^-$. Anal. calcd for $C_{19}H_{23}N_7O_3S_2$: C, 49.44; H, 5.02; N, 21.24; found: C, 49.53; H, 5.09; N, 21.13.

2.1.8. 5-(2-(4-Methylpiperazinyl)-5-(4-methylpiperazinylsulfonyl)-3-thienyl)-1-methyl-3-propyl-1,6-dihydro-7H-pyrazolo[4,3-d]pyrimidin-7-one (11) [32]

After compound **5** (65 mg, 0.13 mmol) was dissolved in DMF (5 mL), $Pd(OAc)_2$ (3 mg, 0.013 mmol), DPPF (14 mg, 0.026 mmol), Cs_2CO_3 (42 mg, 0.13 mmol), and *N*-methylpiperazine (16 mg, 0.16 mmol) were added. The resulted mixture was heated at 120 °C in nitrogen with stirring for 6 h, allowed to cool to room temperature, poured into water, and extracted with ethyl acetate (150 mL). The organic extract was washed with water for three times, dried over Na_2SO_4, and then concentrated in vacuum. The residue was purified by column chromatography (eluted with $CHCl_3$:CH_3OH = 20:1). The yielded compound in title was a white solid (55 mg, yield: 79%).

mp 187–188 °C; ^{1}H NMR (300 MHz, CD_3SOCD_3): δ 0.96 (t, J = 7.2, 3H, CH_3), 1.71–1.78 (m, 2H), 2.19 (s, 3H, NCH_3), 2.23 (s, 3H, NCH_3), 2.43 (br s, 4H), 2.50 (br s, 4H), 2.77 (t, J = 7.2, 2H, CH_2), 3.00 (br s, 4H), 3.13 (br s, 4H), 4.14 (s, 3H, NCH_3), 7.70 (s, 1H), 12.14 (s, 1H); ^{13}C NMR (75 MHz, CD_3SOCD_3): δ 13.82, 21.71, 27.05, 37.74, 45.05, 45.32, 45.63, 52.23, 53.25, 53.68, 117.4, 119.9, 124.0, 134.1, 137.2, 144.5, 145.5, 153.5, 163.1; IR (KBr): 3432, 2940, 1698, 1582 cm^{-1}; ESI-MS: m/z = 533 [M−H]$^-$. Anal. calcd for $C_{23}H_{34}N_8O_3S_2$: C, 51.66; H, 6.41; N, 20.96; found: C, 51.76; H, 6.38; N, 20.91.

2.1.9. 5-(2-Ethoxy-5-(sulfamoyl)-3-thienyl)-1-methyl-3-propyl-1,6-dihydro-7H-pyrazolo[4,3-d]pyrimidin-7-one (12)

Compound **12** was prepared by the same method for compound **8** except for the replacement of methanol and compound **5**, respectively with ethanol and compound **6**. It was a white solid (56 mg, yield: 56%).

mp 255–256 °C; ^{1}H NMR (300 MHz, CD_3SOCD_3): δ 0.94 (t, J = 6.8, 3H, CH_3), 1.46 (t, J = 6.3, 3H), 1.73–1.78 (m, 2H, CH_2), 2.76 (t, J = 7.0, 2H, CH_2), 4.13 (s, 3H, NCH_3), 4.34 (m, 2H, OCH_2), 7.69 (s, 1H), 7.69 (br s, 2H, $SONH_2$), 11.37 (s, 1H); ^{13}C NMR (75 MHz, CD_3SOCD_3): δ 13.79, 14.41, 21.59, 27.10, 37.79, 72.36, 113.7, 123.8, 128.5, 129.6, 137.4, 144.5, 144.6, 153.2, 166.3; IR (KBr): 3332, 3089, 2969, 1684, 1587 cm^{-1}; ESI-MS: m/z = 396 [M−H]$^-$. Anal. calcd for $C_{15}H_{19}N_5O_4S_2$: C, 45.33; H, 4.82; N, 17.62; found: C, 45.29; H, 4.75; N, 17.70.

2.1.10. 5-(5-(Sulfamoyl)-3-thienyl)-1-methyl-3-propyl-1,6-dihydro-7H-pyrazolo[4,3-d]pyrimidin-7-one (13) [27]

To a solution of compound **6** (200 mg, 0.46 mmol) in methanol (20 mL), zinc dust (90 mg, 1.38 mmol) and formic acid (0.2 mL) were added. The mixture was stirred overnight. Excess zinc dust was removed by filtration. The filtrate was concentrated in vacuum and then purified by column chromatography (eluted with $CHCl_3$:CH_3OH = 20:1). The yielded compound in title was a white solid (133 mg, yield: 82%).

mp 307–308 °C; ^{1}H NMR (300 MHz, CD_3SOCD_3): δ 0.95 (t, J = 6.9, 3H, CH_3), 1.73–1.80 (m, 2H), 2.79 (t, J = 7.2, 2H), 4.14 (s, 3H, NCH_3), 7.83 (br s, 2H), 8.15 (s, 1H), 8.63 (s, 1H), 12.51 (br s, 1H); ^{13}C NMR (75 MHz, CD_3SOCD_3): δ 13.78, 21.54, 27.05, 37.77, 124.1, 129.0, 130.4, 134.5, 137.2, 144.6, 145.0, 146.2, 154.1; IR (KBr): 3294, 2958, 1680, 1579 cm^{-1}; ESI-MS: m/z = 352 [M−H]$^-$. Anal. calcd for $C_{13}H_{15}N_5O_3S_2$: C, 44.18; H, 4.28; N, 19.82; found: C, 44.15; H, 4.20; N, 19.86.

2.1.11. 5-(5-(N-Butyloxycarbonylaminosulfonyl)-3-thienyl)-1-methyl-3-propyl-1,6-dihydro-7H-pyrazolo[4,3-d]pyrimidin-7-one (14) [33]

Compound **13** (65 mg, 0.18 mmol) was dissolved in pyridine (4 mL) and 4-dimethylaminopyridine (44 mg, 0.36 mmol) was added. The solution was cooled in ice bath and butyl chloroformate (40 μL, 0.31 mmol) was added. After stirred at room temperature overnight, the mixture was added by HCl (1N, 50 mL) and extracted with ethyl acetate (2× 50 mL). The combined organic layers were washed with HCl (1N) and brine, dried over Na_2SO_4, concentrated in vacuum, and then purified by column chromatography (eluted with $CHCl_3$:CH_3OH = 30:1). The yielded compound in title was a white solid (50 mg, yield: 61%).

mp 317–318 °C (dec.); ^{1}H NMR (500 MHz, CD_3SOCD_3): δ 0.83 (t, J = 7.2, 3H, CH_3), 0.95 (t, J = 6.9, 3H, CH_3), 1.23–1.30 (m, 2H, CH_2), 1.49–1.54 (m, 2H, CH_2), 1.73–1.80 (m, 2H, CH_2), 2.79 (t, J = 7.2, 2H, CH_2), 4.04 (t, J = 5.7, 2H, OCH_2), 4.14 (s, 3H, NCH_3), 8.30 (s, 1H), 8.78 (s, 1H), 12.55 (s, 1H); ^{13}C NMR (125 MHz, CD_3SOCD_3): δ 13.26, 13.69, 18.20, 21.46, 26.97, 29.91, 37.75, 65.75, 124.3, 132.6, 133.8, 134.6, 137.3, 140.5, 144, 8, 144.9, 151.0, 154.2; IR (KBr): 3437, 2961, 1755, 1681, 1584 cm^{-1}; ESI-MS: m/z = 452 [M−H]$^-$. Anal. calcd for $C_{18}H_{23}N_5O_5S_2$: C, 47.67; H, 5.11; N, 15.44; found: C, 47.54; H, 5.17; N, 15.45.

2.1.12. 5-(5-(N-Propyloxycarbonylaminosulfonyl)-3-thienyl)-1-methyl-3-propyl-1,6-dihydro-7H-pyrazolo[4,3-d]pyrimidin-7-one (15)

Compound **15** was prepared from compound **13** by the same procedure for compound **14**, except for a replacement of butyl chloroformate with propyl chloroformate. Yield: 65%.

mp 312–313 °C (dec.); ^{1}H NMR (300 MHz, CD_3SOCD_3): δ 0.84 (t, J = 6.9, 3H, CH_3), 0.95 (t, J = 6.6, 3H, CH_3), 1.52–1.59 (m, 2H, CH_2), 1.72–1.79 (m, 2H, CH_2), 2.79 (t, J = 6.6, 2H, CH_2), 4.00 (t, J = 5.4, 2H, OCH_2), 4.14 (s, 3H, NCH_3), 8.31 (s, 1H), 8.79 (s, 1H), 12.57 (s, 1H); ^{13}C NMR (125 MHz, CD_3SOCD_3): δ 9.84, 13.69, 21.31, 21.47, 26.96, 37.74, 67.50, 124.3, 132.7, 133.8, 134.7, 137.3, 140.5, 144.8, 144.9, 151.0, 154.2; IR (KBr): 3429, 2963, 1748, 1681, 1584 cm^{-1}; ESI-MS: m/z = 438 [M−H]$^-$. Anal. calcd for $C_{17}H_{21}N_5O_5S_2$: C, 46.46; H, 4.82; N, 15.93; found: C, 46.35; H, 4.85; N, 15.87.

2.1.13. 5-(5-(*N*-Isopropyloxycarbonylaminosulfonyl)-3-thienyl)-1-methyl-3-propyl-1,6-dihydro-7H-pyrazolo[4,3-d]pyrimidin-7-one (**16**)

Compound **16** was prepared from compound **13** by the same procedure for compound **14**, except for a replacement of butyl chloroformate with isopropyl chloroformate. Yield: 57%.

mp 309–310 °C (dec.); ^{1}H NMR (500 MHz, CD_3SOCD_3): δ 0.95 (t, J = 6.9, 3H, CH_3), 1.17–1.19 (m, 6H), 1.72–1.79 (m, 2H, CH_2), 2.79 (t, J = 6.9, 2H, CH_2), 4.13 (s, 3H, NCH_3), 4.79–83 (m, 1H, OCH), 8.30 (s, 1H), 8.78 (s, 1H), 12.54 (s, 1H); ^{13}C NMR (125 MHz, CD_3SOCD_3): δ 13.70, 21.32, 21.50, 26.98, 37.75, 70.27, 124.3, 132.7, 133.6, 134.6, 137.3, 140.7, 144.8, 144.9, 150.5, 154.2; IR (KBr): 3444, 2961, 1746, 1682, 1584 cm^{-1}; ESI-MS: m/z = 438 $[M-H]^-$. Anal. calcd for $C_{17}H_{21}N_5O_5S_2$: C, 46.46; H, 4.82; N, 15.93; found: C, 46.55; H, 4.76; N, 15.82.

2.2. Characterization of synthesized inhibitors

Melting points were determined on an X-4 microscopic melting point apparatus (Beijing TaiKe Co. Ltd.). Infrared spectra were recorded on a Thermo Nicolet 330FT-IR spectrophotometer. ^{1}H NMR and ^{13}C NMR spectra were recorded at room temperature in a Varian Mercury-Plus 300 (compounds **4–6**, **8–13**) or Varian INOVA 500NB (compounds **7**, **14–16**), with solvent $CDCl_3$ or CD_3SOCD_3 as the reference for the chemical shifts. Electrospray ionization-mass spectra (ESI-MS) were measured in a Shimadzu LCMS-2010A liquid chromatography mass spectrometer. Flash column chromatography was performed with silica gel (200–300 mesh, Qingdao Haiyang Chemical). Analytical thin-layer chromatography was performed on Merck silica gel GF254 plate. Element analysis was carried out in an Elementar Vario EL.

2.3. Protein expression and purification of PDE5A1

The cDNA of the catalytic domain of human PDE5A1 was generated by the site-directed mutagenesis of the bovine PDE5A gene as previously described [25]. The coding region for amino acids 535–860 of PDE5A1 was amplified by PCR and subcloned into the expression vector pET15b. The resultant plasmid pET-PDE5A1 was transferred into *E. coli* strain BL21 (CodonPlus) for over-expression. The *E. coli* cell carrying pET-PDE5A1 was grown in LB medium at 37 °C to absorption A_{600} = 0.7 and then 0.1 mM isopropyl β-D-thiogalactopyranoside was added for further growth at 15 °C overnight. Recombinant PDE5A1 was passed through a Ni-NTA column (Qiagen), subjected to thrombin cleavage, and further purified by passing through Q-Sepharose and Sephacryl S300 columns (Amersham Biosciences). A typical batch of purification yielded over 10 mg PDE5A1 with a purity >95% from a 2 l cell culture.

The cDNA for expression of the full-length human PDE5A1 (residues 1–875) was a gift from Dr. Corbin at Vanderbilt University and was subcloned into vector pET32a. Protein expression and purification of the full-length PDE5A1 followed a similar protocol for preparation of the catalytic domain of PDE5A1.

2.4. Assay of phosphodiesterase activity

The full-length human PDE5A1 was used to measure the kinetic properties of synthesized inhibitors. PDE5A1 was incubated with a reaction mixture containing 20 mM Tris·HCl, HCl, pH 7.5, 10 mM $MgCl_2$, 0.5 mM DTT, ^{3}H cGMP (20,000 cpm/assay) at room temperature for 15 min. The reaction was terminated by addition of 0.2 M $ZnSO_4$ and 0.2 M $Ba(OH)_2$. The product ^{3}H GMP was precipitated by $BaSO_4$ while unreacted ^{3}H cGMP remained in the supernatant. Radioactivity in the supernatant was measured by liquid scintillation counting. For the measurement of inhibition, at least six concentrations of inhibitors were used together with a substrate concentration at one-tenth of K_M and a suitable enzyme concentration. The IC_{50} values are the concentrations of inhibitors where 50% enzymatic activity is inhibited.

2.5. Protein crystallization and structure determination

The co-crystals of the PDE5A1 (535–860) catalytic domain in complex with compound **12** were grown by vapor diffusion. The PDE5A1–**12** complex was prepared by mixing 1 mM compound **12** with 15 mg/mL PDE5A1 that was stored in a buffer of 20 mM Tris·base, pH 7.5, 50 mM NaCl, 1 mM β-mercaptoethanol, and 1 mM EDTA. The protein drop was prepared by mixing 2 μL protein with 2 μL well buffer and crystallized against a well buffer of 2.0 M sodium formate, 0.1 M sodium citrate, pH 5.6, 5% ethanol at 25 °C. The PDE5A1–**12** crystals had the space group $P3_121$ with cell dimensions of $a = b$ = 73.8 Å and c = 132.5 Å (Table 1). Diffraction data were

Table 1 – Statistics on diffraction data and structure refinement

Data collection	
Space group	$P3_121$
Unit cell [a, b, c (Å)]	73.8, 73.8, 132.5
Resolution (Å)	2.0
Total measurements	243,526
Unique reflections	26,266
Completeness (%)	91.1 (49.8)[a]
Average I/σ	11.0 (2.0)[a]
Rmerge	0.073 (0.35)[a]
Structure refinement	
R-factor	0.197
R-free	0.221 (10%)[b]
Resolution (Å)	30–2.0
Reflections	25,314
RMS deviation for	
Bond (Å)	0.005
Angle (°)	1.2
Average B-factor (Å^2)	
Protein	38.5 (2523)[c]
12	34.1 (26)[c]
Waters	39.6 (116)[c]
Zn	30.4 (1)[c]
Mg	54.4 (1)[c]

[a] The numbers in parentheses are for the highest resolution shell.
[b] The percentage of reflections omitted for calculation of R-free.
[c] The number of atoms in the crystallographic asymmetric unit.

collected on beamline X29 at Brookhaven National Laboratory and processed by program HKL [34].

The PDE5A1–**12** structure was solved by molecular replacement with program AMoRe [35], using the PDE5A1–IBMX structure without the H-loop (residues 660–683) and IBMX as the initial model. The rotation and translation searches for the crystal of PDE5A1–**12** yielded a correlation coefficient of 0.74 and *R*-factor of 0.31 for 3054 reflections between 4 and 8 Å resolution. The atomic model was rebuilt by program O [36] against the electron density maps that were improved by the density modification package of CCP4. The structure was refined by CNS (Table 1) [37].

3. Results

3.1. *Conformational changes of PDE5A1 upon inhibitor 12 binding*

The crystal of PDE5A1 in complex with newly synthesized inhibitor **12** (IC_{50} = 110 nM) contains a monomer of the PDE5A1 catalytic domain (residues 535–860) in the asymmetric unit. Most residues in the PDE5A1–**12** structure have solid electron density and are traced without ambiguity. The PDE5A1–**12** structure consists of 15 α-helices that assemble into a topological fold common to the known structures of PDE5 and the other PDE families (Fig. 2). The structural superposition of PDE5A1–**12** over other PDE5 structures without the H-loop yielded RMSDs of 0.32, 0.32, 0.43, and 0.29 Å, respectively for the unliganded PDE5A1 and its complexes with IBMX, icarisid II, and sildenafil, thus indicating the overall similarity among the PDE5 structures. However, the PDE5A1–**12** structure shows characteristic conformation changes in the H- and M-loops.

The H-loop of PDE5 (residues 660–683) was previously shown to undergo dramatic positional and conformational changes upon inhibitor binding [25]. Four different conformations were identified for the H-loop of PDE5A1: a coil in the unliganded state, two short α-helices in the IBMX complex, a 3_{10} helix in the sildenafil complex, and two short β-strands in the icarisid II complex (Fig. 2). In addition, the H-loops in these complexes showed positional movements of as much as 7, 24, and 35 Å, respectively [25]. The H-loop in the PDE5A1–**12** structure contains 3_{10}- and α-helices at positions 664–667 and 672–676, corresponding to two short α-helices H8 and H9 in the PDE5–IBMX complex [25], but differing from the other PDE5 structures. In addition, the H-loop of PDE5A1–**12** has positional differences of as much as 5 Å from that of the unliganded PDE5A1 and 7 Å from that of the PDE5A1–IBMX structure (Fig. 2). Since the PDE5A1–**12** crystal has similar unit cell parameters and the same space group as the unliganded form and the IBMX complex, the different positions and conformations of the H-loop in these structures must be the consequence of the inhibitor binding, rather than an artifact of crystal packing.

Residues 793–807 of the M-loop, a region spanning the sequence 788–811, are disordered in the PDE5A1–**12** structure, as are those in the unliganded as well as IBMX- and vardenafil-bound structures [25,38]. In contrast, the ordered M-loops in the PDE5–sildenafil and PDE5–icarisid II complexes contact the inhibitors with Leu804 and have similar conformation to those in the structures of other PDE families [4]. A possible explanation for the M-loop disorder in the PDE5A1–**12** structure might be a lack of direct interactions of the inhibitor **12** with the M-loop. However, bound sildenafil and icarisid II might also indirectly enhance the conformational stability of the M-loop by inducing movement of the H-loop and its consequent packing against residues in the M-loop.

3.2. *Binding of inhibitor 12*

Inhibitor **12** binds to a pocket next to the divalent metal ions, but does not directly interact with the metals (Fig. 3). The pyrazolopyrimidinone group of **12** stacks against Phe820 of PDE5A1 and also contacts residues His613, Leu765, Ala767, Ile768, Leu782, Phe786, and Gln817. The O7 and N6 atoms of pyrazolopyrimidinone (Fig. 3) form two hydrogen bonds with Ne2 and Oe1 of Gln817, respectively. The ethoxythiophene group interacts via van der Waals forces with Ala779, Val782, Ala783, Phe786, Met816, Gln817, and Phe820. The ether oxygen of ethoxythiophene is located at a distance of 2.94 Å from the amide oxygen of the Gln817 side chain. This distance suggests an unfavorable interaction because neither oxygen carries a hydrogen donor required for formation of a hydrogen bond. In principle, 180° rotation of the terminal amide of Gln817 might support binding of inhibitor **12** in its hydroxypyrazolopyrimidine tautomeric state. Such a binding mode might then also establish a favorable hydrogen bonded interaction between the inhibitor's ethoxy oxygen and the amide Ne2 of Gln817. The failure to adopt this binding mode may be influenced by the preferential stability of the pyrazolopyrimidinone tautomer of **12** as well the protein's internal hydrogen bonded network that biases the rotameric preferences of Gln817 through interaction with Gln775. Most of the inhibitor's sulfonamide group ($-SO_2NH_2$) makes no contact with the protein, although its nitrogen is located within van der Waals contact distance of the intra-helix carbonyl oxygen of Met816. In addition, two water molecules bind to O7 and N2 of **12** (Fig. 3) and bridge respectively to Ne2 of Gln775 and carbonyl oxygen of Asp764.

The conformation and interaction of inhibitor **12** are comparable with those of sildenafil. Indeed structural superposition between PDE5A1–**12** and PDE5A1–sildenafil shows that the two pyrazolopyrimidinone groups of the inhibitors not only occupy the same position but also have the same conformation (Fig. 3). The thiophene ring of inhibitor **12** co-planes with the phenyl group of sildenafil, but slightly shifts toward the invariant Gln817 (Fig. 3) so that the ethoxy groups of the two inhibitors are superimposed well. As a result, the sulfonamide group shows a significant positional displacement of 1.5 Å between the sulfur atoms of **12** and sildenafil. The binding of the pyrazolopyrimidinone core of **12** also more or less simulates the binding of IBMX, a non-selective PDE inhibitor. The xanthine skeleton of IBMX co-planes with the pyrazolopyrimidinone of **12** and the isobutyl group of IBMX is located in the same pocket as the propyl group of **12** (Fig. 3). Although the orientation of the xanthine is reversed with respect to the pyrazolopyrimidinone of **12**, its O6 and N7 centers occupy roughly the positions of O7 and N6 of the pyrazolopyrimidinone and form two hydrogen bonds with Gln817.

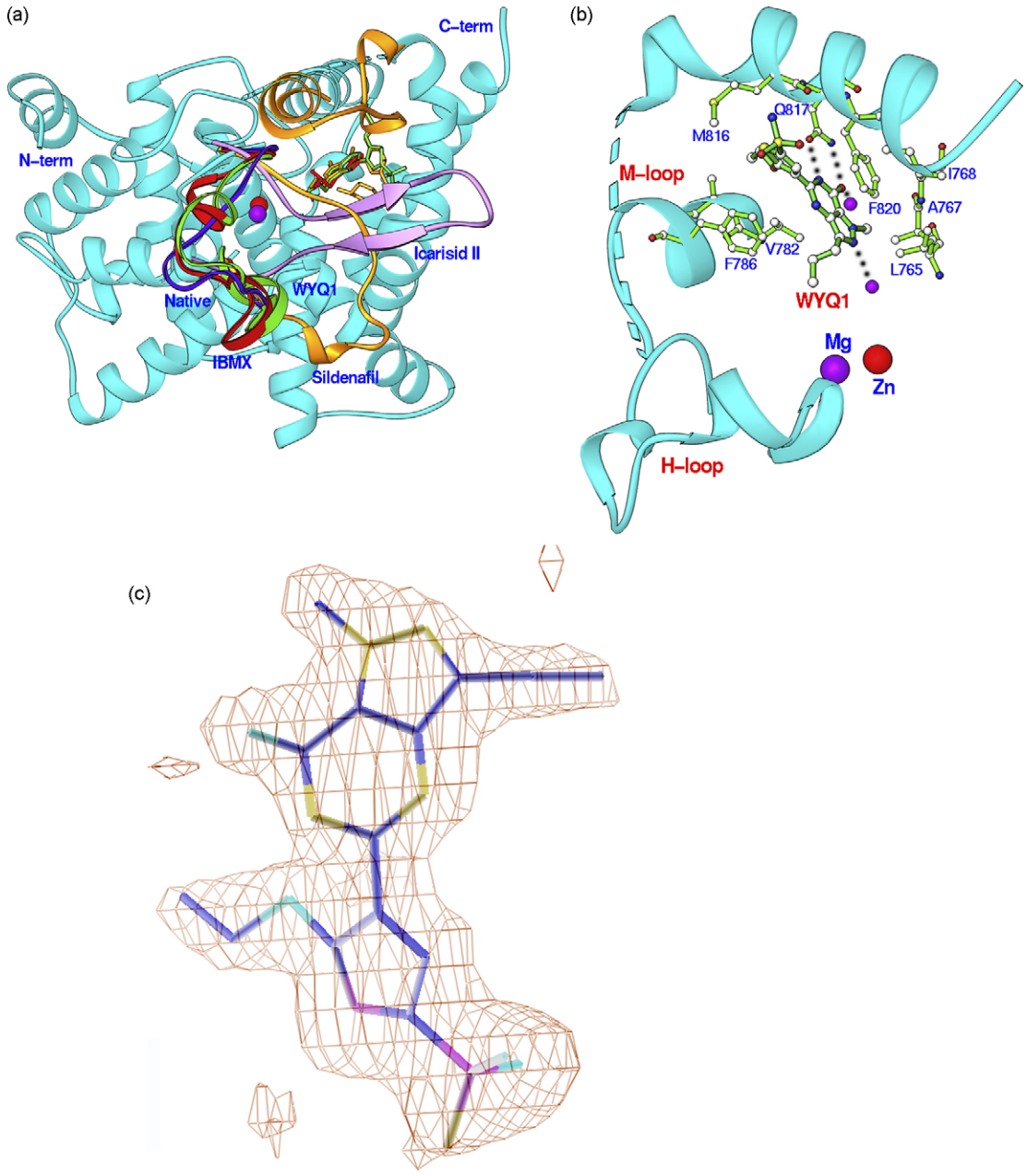

Fig. 2 – PDE5 structures. (a) Ribbon diagram. The cyan ribbons represent the comparable structures of the PDE5 complexes. The H-loops are shown in green for PDE5–12, violet for the unliganded PDE5, red for PDE5–IBMX, light purple for PDE5–icarisid II, and gold for PDE5–sildenafil. (b) Interactions between 12 (labelled as WYQ1) and PDE5 residues. The cyan dotted line represents the disordered M-loop linking helices H14 and H15. The black dotted lines represent the hydrogen bonds. (c) The electron density for compound 12. The (Fo–Fc) map was contoured at three sigmas.

Although the binding of compound **12** causes movement of the H-loop, with atoms displaced as much as 5 Å from their corresponding positions in the unliganded form, the active site in the PDE5A1–**12** structure is still open (Fig. 3), resembling that of the unliganded or IBMX-bound forms. The solvent accessible area of **12** is 18.5%. In comparison, sildenafil induces profound movement of the H-loop as much as 24 Å from that in the unliganded PDE5 structure. As a result, the active site of PDE5A1 is transformed into a closed form and sildenafil is buried in the pocket, with a solvent accessible surface of only 9.4% [25].

3.3. *Structure and activity relationships suggest that a hydrophobic pocket is critical for the PDE5 inhibitor binding*

Internal and external bond angles for a symmetrical five-membered ring are respectively 108° and 126°, whereas the corresponding angles for a six-membered ring are 120°. The bond angle difference between five- and six-membered rings might, in principle, relax oxygen–oxygen opposition between the sildenafil ethoxy group and Gln817 upon replacement of the inhibitor's ethoxyphenyl by an ethoxythiophene subunit.

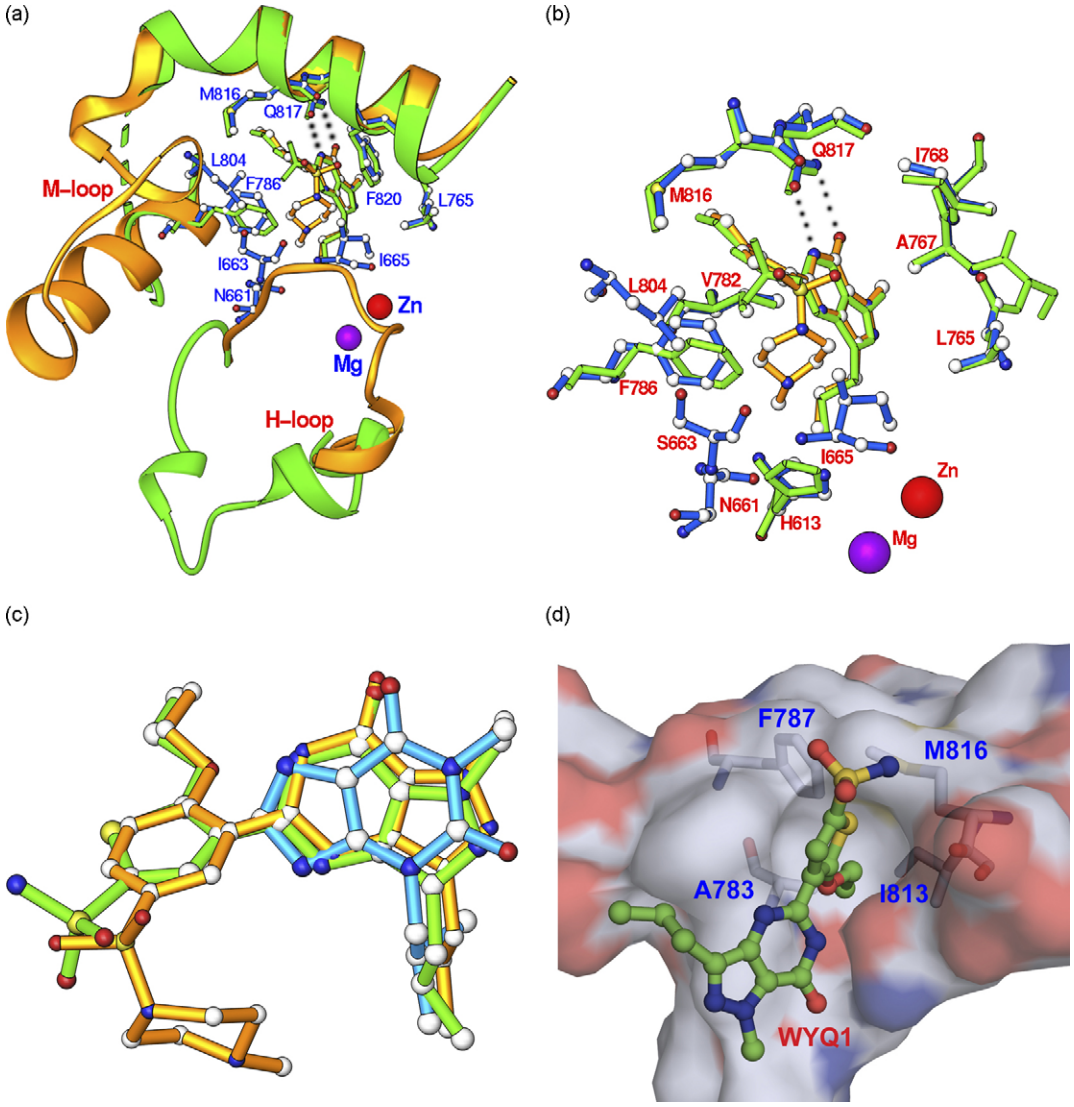

Fig. 3 – Binding and comparison of the PDE5 inhibitors. (a) Structural superposition of PDE5A1–12 (green ribbons and bonds) over PDE5A1–sildenafil (golden ribbons and blue bonds). The M-loop is disordered in PDE5A–12. (b) Detailed view of the superposition. Leu804 interacts with sildenafil but disordered in PDE5A–12. Residues Asn661, Ser663, and Ile665 of the H-loop interact with sildenafil, but have different location in the PDE5A1–12 structure and do not contact compound 12. (c) Superposition of compound 12 (green bond) over sildenafil (gold) and IBMX (cyan). The pyrazolopyrimidinone is co-planed with xanthine of IBMX. The sulfonamide of 12 shows as much as 1.5 Å positional displacement. (d) A surface presentation of a small hydrophobic pocket for the binding of the ethoxy group of the PDE5 inhibitors.

Such a replacement might therefore be expected to improve the interaction with Gln817 if other parts of the structure remain unchanged. In contrast to this expectation, the direct thiophene-for-phenyl replacement analogue, compound **9** (IC_{50} = 1350 nM, Table 2), showed far weaker affinity as an inhibitor than the parent sildenafil (IC_{50} = 3.5 nM), with a 386-fold loss of activity. To explore the basis for this unexpected affinity deterioration, the pharmacophore was investigated by variation of thiophene ring substituents R1 and R2 for structure–activity analysis.

When R2 is $–NH_2$, compound **12** with R1 = –OEt has about 60-fold better affinity than compound **13** that has R1 = –H (Table 2). This affinity difference could be explained on the basis of the crystal structures [21–25], in which R1 orients to a small hydrophobic pocket comprising residues Glu780, Ala783, Phe787, Ile813, and Met816 (Fig. 3d). Thus, the van der Waals contact of the ethyl group with the pocket will significantly enhance the binding affinity. The significance of this hydrophobic interaction is further emphasized by comparison of UK-122764 and sildenafil. UK-122764 lacks the piperazine-sulfonamide tail, but has a propyl group in the place of the ethyl group (Fig. 1). Since the methylpiperazine of sildenafil forms van der Waals interactions with Asn662, Ser663, Tyr664, Ile665, Leu804, and Phe820 in the crystal structure of PDE5A1–sildenafil [25], truncation of the extended tail subunit in UK-122764 would be expected to result in significant loss of affinity. However, the IC_{50} of UK-122764 is only fivefold weaker than that of sildenafil

Table 2 – IC_{50} of PDE5 inhibitors with thiophene ring

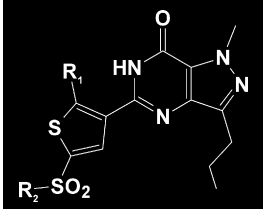

Inhibitors	R1	R2	IC_{50} (μM)
7	H		0.48
8	MeO–		16.1
9	EtO–		1.35
10	NC–		5.9
11			13.6
12	EtO–	NH_2	0.11
13	H	NH_2	6.5
14	H	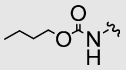	1.7
15	H	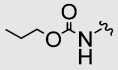	1.7
16	H		2.2
Sindenafil			0.0035

[39,40]. This unexpected affinity change of UK-122764 might be attributed to the better fit of the propyl group than the ethyl group in the small hydrophobic pocket. Therefore, optimal occupancy of this small hydrophobic pocket is a key determinant for high binding affinity of PDE5 inhibitors.

When R2 is methylpiperazine, compound **7** (R1 = –H) shows higher affinity than compounds **8**–**11** (Table 2). The weak binding of compound **11** can be simply explained by the fact that R1 = methylpiperazine is too large to fit into the small hydrophobic pocket (Fig. 3d). However, the factors underlying the observed structure–IC_{50} relationship for compounds **7**–**10** are complicated. Apparently, R1 is involved in two types of interactions: hydrophobic interaction with the small pocket and a polar contact with the invariant glutamine. Thus, a suitably sized hydrocarbon chain in R1 would be expected to favor binding of the compound, as seen with compound **9**, where inhibitory potency is slightly better than compounds **8**, **10**, and **11**. The absence of a substituent at the R1 position will tend to compromise affinity by loss of favorable interactions within the hydrophobic pocket. On the other hand, the absence of this group also relieves repulsion with Gln817 (Fig. 1), offsetting the loss in affinity caused by removal of the contact with the hydrophobic pocket. These factors combine to give a threefold affinity difference between compounds **7** and **9**. In short, the interaction of R1 with the small hydrophobic pocket and also with the invariant glutamine is important for affinity of PDE5 inhibitors.

3.4. *Conformational change of the H-loop is apparently a factor for PDE5 inhibition*

The structural studies of this PDE5–**12** and other PDE5 complexes [25] suggest that conformational and positional changes of the H-loop are involved in the mechanism of PDE5 inhibition and function. The H-loops in the unliganded state and in the **12**- or IBMX-bound structures occupy similar locations, but have relative displacements of several Angstroms and different conformations. Since these weakly bound inhibitors do not directly contact the H-loop, the conformational changes of the H-loop must be achieved via an allosteric mode, although the exact path needs further study. In contrast, the large inhibitors, icarisid II and sildenafil, directly interact with and drag the H-loop to cover up the catalytic pocket. This modification of the active site inactivates PDE5 and may thus impact on the *in vivo* function of PDE5.

The structure–activity study suggests that the conformation and position of the H-loop are a factor for the function of PDE5 inhibitors, in addition to pi-stacking of inhibitors against the conserved phenylalanine and hydrogen bonding to the invariant glutamine [4,22,25]. When R1 is a hydrogen atom, the inhibitors with a large substituent at the R2 position have better affinity, as shown by 3.5–13-fold higher affinity of compound **7** over compounds **13**–**16** (Table 2). This might be explained by the van der Waals interactions of the methylpiperazine group with the H-loop residues of Asn662, Ser663, Tyr664, Ile665, as well as with Leu804 and Phe820 in a manner similar to the interactions of sildenafil in the crystal structure of PDE5A1–sildenafil [25]. However, when R1 is an ethoxy group, compound **12** with R2 = $–NH_2$ has about 12-fold better affinity than compound **9** that has R2 = methylpiperazine. The explanation of this inconsistent contribution of the tail is not clear. While the sulfonamide ($–SO_2NH_2$) nitrogen of **12** makes favorable van der Waals interactions with the carbonyl oxygen of Met816, compound **9** might not be able to form the same contact so as to cause the loss of 12-fold affinity. Since the majority of residues interacting with the tails of the inhibitors come from the H-loop, the position and conformation of the H-loop must be a factor for affinity of PDE5 inhibitors. This assumption is supported by the observation that the H-loop in the PDE5 structure in complex with vardenafil, which has similar chemical structure but substantially higher affinity than sildenafil, showed dramatically different conformation from that in the PDE5–sildenafil structure [38]. Clearly the M-loop also contributes to the binding of extended inhibitor structures, as shown by the interaction of Leu804 with both sildenafil and icarisid II. Given that the H-loop folds over the M-loop in the co-crystal structures of these latter compounds with PDE5, it is likely that the interactions between bound inhibitor and residues in the two loops are not independent.

4. Discussion

While the PDE5 inhibitors sildenafil, vardenafil, and tadalafil have been successfully used to treat erectile dysfunction, interest continues in the development of second generation PDE5 inhibitors for new applications such as cancer and cardiovascular disease. The structure–activity study in this paper suggests that the conformational variation of the H-loop and a small hydrophobic pocket are two factors for PDE5 inhibitor binding, in addition to two common elements of the hydrophobic stack against the phenylalanine and the hydrogen bonds with the invariant Gln817 [4]. However, the structural information of PDE5–**12** could not fully explain all the observed changes in inhibitory potency of the compounds in this study. For example, the substitution of EtO for H in R1 when R2 consists of the piperazine group (compounds **13**–**12** in Table 2) generates a 60-fold increase in affinity. This could apparently be explained with the ''hydrophobic pocket'' stabilizing the EtO group. However, the same substitution in R1 when R2 consists of a piperazine group (compounds **7** and **8**) causes a threefold decrease in affinity, inconsistent with the simple hydrophobic model. Another example is the 390-fold loss in binding affinity of analogue **9** in comparison to its parent sildenafil, resulting from the substitution of the thiophene ring. The structural comparison of the inhibitors (Fig. 3c) suggests that the five-membered ring of **12** superimposed well with the six-membered ring of sildenafil, but caused 1.5 Å positional movement of the sulfur atom of the sulfonamide group. However, this shift does not appear to generate obvious steric constraints that would prevent the piperazine ring of inhibitor **9** from occupying similar space for the corresponding sildenafil ring. Therefore, other explanations are open. For example, optimal interactions of the piperazine-sulfonamide tail with the H- and M-loops cannot be achieved in the inhibitors with the five-membered ring whilst accommodating the ethoxy group to balance the favorable interactions in the hydrophobic pocket against the unfavorable contact with Gln817. Another element for the inhibitor affinity may be the conformational change of the M-loop and possible corporative conformational changes of the H- and M-loops. However, the disorder of the M-loop in the PDE5–**12** structure does not allow a rational explanation, and thus further structural studies are needed.

In short, analysis of the structure and affinity relationships for compounds **7**–**16** suggests that the six-membered phenyl ring in sildenafil is the key to correctly positioning the sulfonamide group and is thus required for high affinity binding to PDE5. Since the five-membered thiophene replacement does not improve the interaction with the invariant glutamine, repositioning the ethoxy group from the *ortho*- to the *meta*-position of the phenyl ring would be a future consideration to keep the favored hydrophobic interaction, but avoid of the repulsion with the glutamine.

Accession code

The coordinates and structural factors have been deposited into the Protein Data Bank with accession code of 3BJC.

Acknowledgements

We thank beamline X29 at NSLS for collection of diffraction data. This work was supported by NIH GM59791 to HK and by the 985 project and Science Foundation of Sun Yat-Sen University.

REFERENCES

[1] Bender AT, Beavo JA. Cyclic nucleotide phosphodiesterases: molecular regulation to clinical use. Pharmacol Rev 2006;58:488–520.
[2] Lugnier C. Cyclic nucleotide phosphodiesterase (PDE) superfamily: a new target for the development of specific therapeutic agents. Pharmacol Ther 2006;109:366–98.
[3] Omori K, Kotera J. Overview of PDEs and their regulation. Circ Res 2007;100:309–27.
[4] Ke H, Wang H. Crystal structures of phosphodiesterases and implications on substrate specificity and inhibitor selectivity. Curr Top Med Chem 2007;7:391–403.
[5] Conti M, Beavo J. Biochemistry and physiology of cyclic nucleotide phosphodiesterases: essential components in cyclic nucleotide signaling. Ann Rev Biochem 2007;76: 481–511.
[6] Truss MC, Stief CG, Uckert S, Becker AJ, Wafer J, Schultheiss D, et al. Phosphodiesterase 1 inhibition in the treatment of lower urinary tract dysfunction: from bench to bedside. World J Urol 2001;19:344–50.
[7] Rotella DP. Phosphodiesterase 5 inhibitors: current status and potential applications. Nat Rev Drug Discov 2002;1: 674–82.
[8] Schrör K. The pharmacology of cilostazol. Diabetes Obes Metab 2002;4(suppl. 2):S14–9.
[9] Abdel-Hamid IA. Phosphodiesterase 5 inhibitors in rapid ejaculation: potential use and possible mechanisms of action. Drugs 2004;64:13–26.
[10] Lipworth BJ. Phosphodiesterase-4 inhibitors for asthma and chronic obstructive pulmonary disease. Lancet 2005;365:167–75.
[11] Castro A, Jerez MJ, Gil C, Martinez A. Cyclic nucleotide phosphodiesterases and their role in immunomodulatory responses: advances in the development of specific phosphodiesterase inhibitors. Med Res Rev 2005;25:229–44.
[12] Houslay MD, Schafer P, Zhang KY. Keynote review: phosphodiesterase-4 as a therapeutic target. Drug Discov Today 2005;10:1503–19.
[13] Blokland A, Schreiber R, Prickaerts J. Improving memory: a role for phosphodiesterases. Curr Pharm Des 2006;12: 2511–23.
[14] Menniti FS, Faraci WS, Schmidt CJ. Phosphodiesterases in the CNS: targets for drug development. Nat Rev Drug Discov 2006;5:660–70.
[15] Galie N, Ghofrani HA, Torbicki A, Barst RJ, Rubin LJ, Badesch D, et al. Sildenafil citrate therapy for pulmonary arterial hypertension. N Engl J Med 2005;353:2148–57.
[16] Salem EA, Kendirci M, Hellstrom WJ. Udenafil a long-acting PDE5 inhibitor for erectile dysfunction. Curr Opin Invest Drugs 2006;7:661–9.
[17] Supuran CT, Mastrolorenzo A, Barbaro G, Scozzafava A. Phosphodiesterase 5 inhibitors—drug design and differentiation based on selectivity, pharmacokinetic and efficacy profiles. Curr Pharm Des 2006;12:3459–65.
[18] Stehlik J, Movsesian MA. Inhibitors of cyclic nucleotide phosphodiesterase 3 and 5 as therapeutic agents in heart failure. Expert Opin Invest Drugs 2006;15:733–42.

[19] Palmer MJ, Bell AS, Fox DN, Brown DG. Design of second generation phosphodiesterase 5 inhibitors. Curr Top Med Chem 2007;7:405–19.
[20] Zhu B, Strada SJ. The novel functions of cGMP-specific phosphodiesterase 5 and its inhibitors in carcinoma cells and pulmonary/cardiovascular vessels. Curr Top Med Chem 2007;7:437–54.
[21] Sung BJ, Hwang KY, Jeon YH, Lee JI, Heo YS, Kim JH, et al. Structure of the catalytic domain of human phosphodiesterase 5 with bound drug molecules. Nature 2003;425:98–102.
[22] Huai Q, Liu Y, Francis SH, Corbin JD, Ke H. Crystal structures of phosphodiesterases 4 and 5 in complex with inhibitor IBMX suggest a conformation determinant of inhibitor selectivity. J Biol Chem 2004;279:13095–101.
[23] Zhang KY, Card GL, Suzuki Y, Artis DR, Fong D, Gillette S, et al. Glutamine switch mechanism for nucleotide selectivity by phosphodiesterases. Mol Cell 2004;15:279–86.
[24] Card GL, England BP, Suzuki Y, Fong D, Powell B, Lee B, et al. Structural basis for the activity of drugs that inhibit phosphodiesterases. Structure 2004;12:2233–47.
[25] Wang H, Liu Y, Huai Q, Cai J, Zoraghi R, Francis SH, et al. Multiple conformations of phosphodiesterase-5: implications for enzyme function and drug development. J Biol Chem 2006;281:21469–7.
[26] Rotella DP, Sun Z, Zhu Y, Krupinski J, Pongrac R, Seliger L, et al. *N*-3-Substituted imidazoquinazolinones: potent and selective PDE5 inhibitors as potential agents for treatment of erectile dysfunction. J Med Chem 2000;43:1257–63.
[27] Mader MM, Shih C, Considine E, Dios AD, Grossman CS, Hipskind PA, et al. Acyl sulfonamide anti-proliferatives. Part 2. Activity of heterocyclic sulfonamide derivatives. Bioorg Med Chem Lett 2005;15:617–20.
[28] El-Abadelah MM, Sabri SS, Khanfar MA, Voelter W, Abdel-Jalil RJ, Maichle-Mossmer C, et al. Synthesis and properties of a-thiagra. A substituted 5-(2-thienyl)pyrazolo[4,3-*d*]pyrimidin-7-one bioisostere of Viagra. Heterocycles 2000;53:2643–52.
[29] Dale DJ, Dunn PJ, Golightly C, Hughes ML, Levett PC, Pearce AK, et al. The chemical development of the commercial route to sildenafil: a case history. Org Process Res Develop 2000;4:17–22.
[30] Keegstra MA, Peters THA, Brandsma L. Copper(I) halide catalyzed synthesis of alkyl aryl and alkyl heteroaryl ethers. Tetrahedron 1992;48:3633–52.
[31] El Kassmi A, Fache F, Lemaire MA. convenient synthesis of 3-fluorothiophene. Synth Commun 1994;24:95–101.
[32] Mann G, Hartwig JF, Driver MS, Fernández-Rivas C. Palladium-catalyzed C–N(sp_2) bond formation: *N*-arylation of aromatic and unsaturated nitrogen and the reductive elimination chemistry of palladium azolyl and methyleneamido complexes. J Am Chem Soc 1998;120: 827–8.
[33] Wu X, Wan Y, Mahalingam AK, Murugaiah AMS, Plouffe B, Botros M, et al. Selective angiotensin II AT2 receptor agonists: arylbenzylimidazole structure–activity relationships. J Med Chem 2006;49:7160–8.
[34] Otwinowski Z, Minor W. Processing of X-ray diffraction data collected in oscillation mode. Methods Enzymol 1997;276:307–26.
[35] Navaza J, Saludjian P. AMoRe: an automated molecular replacement program package. Methods Enzymol 1997;276:581–94.
[36] Jones TA, Zou J-Y, Cowan SW, Kjeldgaard M. Improved methods for building protein models in electron density maps and the location of errors in these models. Acta Crystallogr A 1991;47:110–9.
[37] Brünger AT, Adams PD, Clore GM, DeLano WL, Gros P, Grosse-Kunstleve RW, et al. Crystallography & NMR system: a new software suite for macromolecular structure determination. Acta Crystallogr D 1998;54:905–21.
[38] Wang H, Ye M, Robinson H, Francis SH, Ke H. Conformational variations of both PDE5 and inhibitors provide the structural basis for the physiological effects of vardenafil and sildenafil. Mol Pharmacol 2008;73: 104–10.
[39] Turko IV, Francis SH, Corbin JD. Hydropathic analysis and mutagenesis of the catalytic domain of the cGMP-binding cGMP-specific phosphodiesterase (PDE5). cGMP versus cAMP substrate selectivity. Biochemistry 1998;37:4200–5.
[40] Turko IV, Ballard SA, Francis SH, Corbin JD. Inhibition of cyclic GMP-binding cyclic GMP-specific phosphodiesterase (Type 5) by sildenafil and related compounds. Mol Pharmacol 1999;56(1):124–30.